286

Optics Communications 91 (1992) 229-235
North-Holland

OPTICS
COMMUNICATIONS

# A side-pumped Nd:YAG epitaxial waveguide laser

D.C. Hanna, A.C. Large, D.P. Shepherd, A.C. Tropper
*Department of Physics and Optoelectronics Research Centre, University of Southampton, Highfield, Southampton SO9 5NH, UK*

I. Chartier, B. Ferrand and D. Pelenc
*LETI/DOPT/CEA-CENG 85 X, 38 041 Grenoble, Cedex, France*

Received 6 March 1992

We report the first operation of a side-pumped crystal waveguide laser. Both diode array and dye laser side-pumping of an epitaxially grown Nd:YAG planar waveguide laser have been demonstrated, with thresholds as low as 8 mW observed for a simple plane mirror cavity. Output slope efficiencies of 19% have also been demonstrated. The threshold and slope efficiency of this system is found to be in good agreement with a simple analytical model.

## 1. Introduction

The advantages that can be offered by doped optical waveguides, including very low laser thresholds and high performance amplifiers, have been clearly demonstrated in glass optical fibres [1]. Recently much work has also been carried out on waveguide lasers based on crystal hosts because these materials offer a wide range of interesting possibilities, such as broadly tunable operation [2,3,4] and upconversion lasing [5,6]. Some crystal hosts also offer nonlinear and/or electro-optic properties which allow internal second harmonic generation and integrated modulation [7,8]. Many techniques can be used to form crystal waveguide lasers, including ion-implantation [9,10], proton exchange [11], Ti-indiffusion [12] and crystal fibre growth [13]. Liquid-phase epitaxial growth [14] offers another technique which can be applied to a wide range of different crystals and has recently been used to produce an exceptionally low loss planar Nd:YAG waveguide laser [15].

A typical pumping arrangement for such waveguide lasers has been longitudinally pumping by single stripe diode lasers, thus limiting the output to rather low average powers at present. An exception to this is the cladding-pumping scheme, demonstrated for fibre lasers, which allows efficient end pumping with a high power diode array [16]. For diode-array-pumped bulk (unguided) crystal lasers there have been numerous reports of both end pumping and side pumping, including a hybrid arrangement referred to as the tightly folded resonator [17]. Here we report the first side-pumped crystal waveguide laser, using both dye laser and diode array pumping. The waveguide used is the same as that used in the longitudinally pumped experiments of ref. [15]. Our results confirm that the planar waveguide geometry is well suited to this transverse pumping arrangement, with the tight pump confinement leading to a low threshold and good slope efficiency. The simplicity of this pumping arrangement suggests that a rugged compact system should be feasible with multiwatt performance when pumped by diode bars. A simple theory of laser threshold and slope efficiency for such a side-pumped system is developed and shown to be in good agreement with our experimental results. This theory suggests that for an optimised system diode-pumped slope efficiencies of ~30% should be obtained.

## 2. Waveguide properties

The fabrication details of the waveguide used in these experiments are described in ref. [15]. The guide consists of a 38 μm deep layer of 1.5 at% $Nd^{3+}$

doped YAG grown by liquid phase epitaxy on an undoped YAG substrate. A 60 μm layer of undoped YAG is then grown on top of this to act as a cladding. The guide was cut and polished to a length of 6 mm as in ref. [15], but this time the side face was also polished to allow side-pumping. The refractive index difference between the doped and undoped layers is sufficient to provide waveguide confinement in the Nd:YAG layer. This guide was multimode at the signal wavelength of 1.064 μm and had a fundamental mode spot size ($1/e^2$ half width of intensity) of 14 μm, indicating good confinement within the physical dimensions of the doped layer. From the laser threshold obtained with longitudinal pumping an upper limit of 0.05 dB/cm can be placed upon the propagation loss, which is near to that of bulk Nd:YAG.

## 3. Theory of laser threshold and slope efficiency

The threshold pump power $P_{\mathrm{pth}}$ and slope efficiency $\eta$ for a laser-pumped four-level laser is given by [18]

$$P_{\mathrm{pth}} = \frac{h\nu_{\mathrm{p}} L}{\eta_{\mathrm{q}} W \sigma \tau_{\mathrm{f}} [1-\exp(-\alpha_{\mathrm{p}} l)]} \times \left( \int_{\mathrm{Cavity}} r_0(x,y,z)\, s_0(x,y,z)\, \mathrm{d}V \right)^{-1} \qquad (1)$$

and

$$\eta = \frac{T\nu_{\mathrm{l}}}{2L\nu_{\mathrm{p}}} [1-\exp(-\alpha_{\mathrm{p}} l)] \eta_{\mathrm{q}} \eta_{\mathrm{pl}} , \qquad (2)$$

where $\nu_{\mathrm{p}}$ is the pump frequency, $\nu_{\mathrm{l}}$ is the laser frequency, $L$ is the single pass loss, $\sigma$ is the emission cross-section, $\tau_{\mathrm{f}}$ is the fluorescence lifetime, $\eta_{\mathrm{q}}$ is the pumping quantum efficiency, $W$ is the length of the medium in the lasing direction, $l$ is the length of the medium in the pumping direction, $\alpha_{\mathrm{p}}$ is the pump absorption coefficient and $T$ is the output mirror transmission. The factor $\eta_{\mathrm{pl}}$ modifies the plane wave expression for $\eta$ and for low power operation ($s_{\mathrm{e}}/I_0 \ll 1$, where $s_{\mathrm{e}}$ is the steady-state photon density and $I_0 = 1/c_{\mathrm{n}}\sigma\tau_{\mathrm{fl}}$ [18]) is given by

$$\eta_{\mathrm{pl}} = \left( \int_{\mathrm{Cavity}} r_0(x,y,z)\, s_0(x,y,z)\, \mathrm{d}V \right)^2 \times \left( \int_{\mathrm{Cavity}} r_0(x,y,z)\, s_0^2(x,y,z)\, \mathrm{d}V \right)^{-1} . \qquad (3)$$

The normalised pump-rate per unit volume, $r_0$, and photon density, $s_0$, are defined by

$$\int_{\mathrm{Cavity}} r_0(x,y,z)\, \mathrm{d}V = \int_{\mathrm{Cavity}} s_0(x,y,z)\, \mathrm{d}V = 1 . \qquad (4)$$

Figure 1 shows the system being modelled. The integration for $r_0$ is carried out over the limits 0 to $W$ (for $z$), $-d$ to $d$ (for $y$), and 0 to 1 (for $x$) as this defines the doped region. The limits used for $s_0$ are the same except for the $y$ direction where limits of $-\infty$ to $\infty$ are used since the signal mode can extend outside the doped region. However the large index difference between the crystal and air will give very strong confinement in the $x$ direction so the limits 0 to 1 are retained. Thus assuming single mode gaussian profiles in the vertical ($y$) and horizontal ($x$) dimensions, and also assuming the spot sizes do not vary as they propagate, we obtain the following,

$$r_0 = \frac{4\alpha_{\mathrm{p}}}{\pi W_{\mathrm{pz}} W_{\mathrm{py}} [1-\exp(-\alpha_{\mathrm{p}} l)]} \times \exp\left[ -\left( \frac{2y^2}{W_{\mathrm{py}}^2} + \frac{2z^2}{W_{\mathrm{pz}}^2} + \alpha_{\mathrm{p}} x \right) \right] \times \left[ \mathrm{erf}\left( \frac{\sqrt{2}d}{W_{\mathrm{py}}} \right) \mathrm{erf}\left( \frac{\sqrt{2}W}{W_{\mathrm{pz}}} \right) \right]^{-1} \qquad (5)$$

and

$$s_0 = \frac{4}{\pi W_{\mathrm{ly}} W_{\mathrm{lx}} W} \exp\left[ -\left( \frac{2(x-a)^2}{W_{\mathrm{lx}}^2} + \frac{2y^2}{W_{\mathrm{ly}}^2} \right) \right] \times \left[ \mathrm{erf}\left( \frac{\sqrt{2}l}{W_{\mathrm{lx}}} - \frac{\sqrt{2}a}{W_{\mathrm{lx}}} \right) + \mathrm{erf}\left( \frac{\sqrt{2}a}{W_{\mathrm{lx}}} \right) \right]^{-1} , \qquad (6)$$

where $a$ is the distance between the edge of the crystal and the centre of the signal mode profile (in the $x$ direction). Combining eqs. (1), (2), (3), (5), and (6) leads to

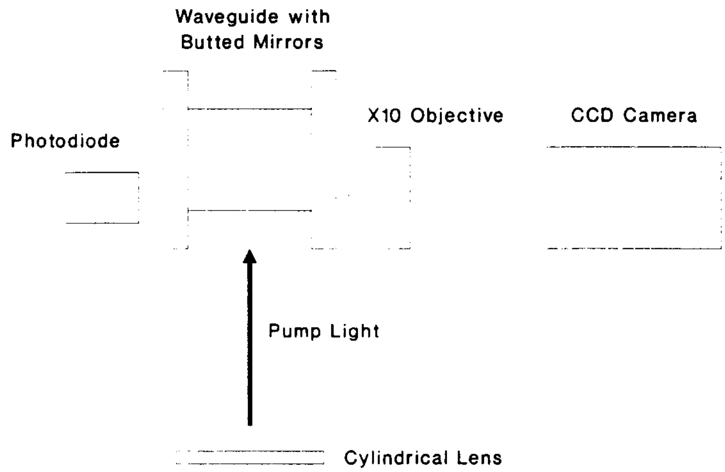


Fig. 2. Schematic diagram of the experimental arrangement for the side-pumped waveguide laser.

gave poor results in this case, possibly due to non-uniform butting of the mirror over the large, horizontal (unguided) mode profile. We have therefore resorted to using large mirrors (without any liquid) close to the waveguide ends but not in actual contact with them. Since the mode size is relatively large (14 μm) the consequent diffraction loss is not significant. For optimised performance, direct coating of the guide end-faces would obviously be preferred. The light output was monitored from both ends of the waveguide by a large area photodiode to observe when lasing occurred and a CCD camera connected to an image analyzer to observe the output profile. Using high reflectivity mirrors, laser action occurred at a power of 10 mW incident upon the 5 cm lens. Taking into account the measured lens transmission (90%), the Fresnel loss at the YAG side face (8%), and assuming 100% launch efficiency we obtain a launched power threshold of ~8 mW. Near threshold the output is observed to be a single gaussian mode in both planes with spot sizes of 14 μm and 140 μm in the vertical and horizontal planes respectively. Figure 3 shows a 3D plot of the imaged output profile observed with the CCD camera. It is also possible to see the top and side edges of the crystal with the camera (although they are less clearly visible in the 3D plot), and it can be seen that the output beam is formed very close to the side edge where the pump beam enters. This is typical of the output profile when the mirrors are adjusted for optimum threshold.

The absorption length of the dye laser pump was measured by directing the beam through the large, 6 mm by 5 mm, faces perpendicular to the plane of the guide. From the transmission measurement over the known depth of the guide (there is a guide on both the top and bottom surfaces) and accounting for Fresnel losses we find an absorption length of ~330 μm. Thus the laser mode with its 140 μm radius (at the $1/e^2$ point of intensity) laser mode should have a reasonable overlap with the pumped volume, although it is not at the optimum condition mentioned earlier ($W_{Lr}=0.83 l_{abs}$).

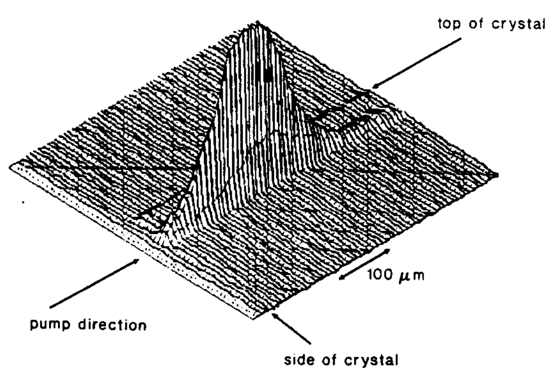


Fig. 3. 3D plot of the imaged output profile of the side-pumped waveguide laser near threshold.

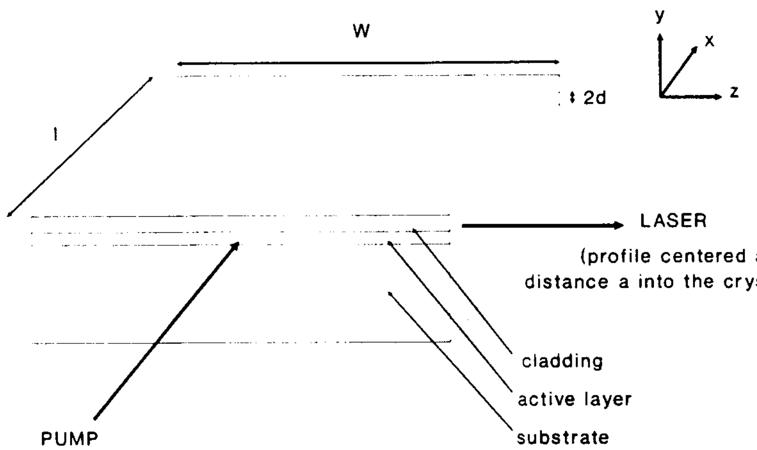


Fig. 1. Model for the side-pumped waveguide system.

$$P_{\mathrm{pth}} = \frac{k\sqrt{\pi} h\nu_{\mathrm{p}} L}{\sqrt{2}\sigma\tau_{\mathrm{f}}\eta_{\mathrm{q}}\alpha_{\mathrm{p}}} (W_{\mathrm{l}y}^2 + W_{\mathrm{p}y}^2)^{1/2} \times \exp(a\alpha_{\mathrm{p}} - W_{\mathrm{L}x}^2 \alpha_{\mathrm{p}}^2/8) \quad (7)$$

and

$$\eta = \frac{k'\sqrt{\pi} T\nu_{\mathrm{l}}\eta_{\mathrm{q}}}{2L\nu_{\mathrm{p}}} \frac{\alpha_{\mathrm{p}} W_{\mathrm{L}x} W_{\mathrm{l}y} (W_{\mathrm{l}y}^2 + 2W_{\mathrm{p}y}^2)^{1/2}}{W_{\mathrm{l}y}^2 + W_{\mathrm{p}y}^2} \times \exp(3W_{\mathrm{L}x}^2\alpha_{\mathrm{p}}^2/16 - a\alpha_{\mathrm{p}}) , \quad (8)$$

where $k$ and $k'$ are factors containing error functions arising from our choice of integration limits and are stated in the appendix. For all practical situations $k$ and $k'$ are close to unity and indeed if the integration limits over $x$ and $y$ are changed to $\pm\infty$ we obtain the same as eqs. (7) and (8) without these factors present.

If we assume that the laser intensity falls to $\sim 0$ at the edge of the crystal such that $3W_{\mathrm{L}x} = 2a$ (equivalent to the condition for transmitting $\sim 99\%$ of a gaussian profile beam through an aperture) we find that the factor $\eta_{\mathrm{pl}}$ has an optimum value of 0.415 when $W_{\mathrm{L}x} = 0.83 l_{\mathrm{abs}}$ (where $l_{\mathrm{abs}} = 1/\alpha_{\mathrm{p}}$). Thus we can predict a maximum possible slope efficiency of 31.5% (0.415 multiplied by the ratio of the signal and pump wavelengths) for diode side-pumping of this system, e.g. in principle one could obtain 1.5 W of output when pumping with a 5 W diode bar. Double-sided-pumping or reflecting the pump after $\sim \frac{1}{2} l_{\mathrm{abs}}$ should further improve the possible slope efficiency by producing a more uniform inversion density distribution.

## 4. Experimental results

While our ultimate interest was in the performance under diode array pumping, our initial trials were carried out using an R6G dye laser as the pump source. In fact, using the $\sim 590$ nm pump wavelength with its shorter absorption length than for the 807 nm output of the diode gives useful information on how the side-pumped performance varies with absorption strength and hence gives some indication of what should be optimum $Nd^{3+}$ doping level in future experiments. The experimental set-up is shown schematically in fig. 2 where the pump beam travels in the plane of the waveguide. The pump light was focused in the vertical (guided) plane with a 5 cm focal length cylindrical lens, to produce a $\sim 7$ μm waist spot size at the entrance to the polished side face of the guide. The beam was unfocused in the horizontal plane having a spot size of 1.25 mm. In previous experiments with crystal waveguide lasers the cavity has usually been formed with two plane mirrors butted against the waveguide ends. Damage to the crystal end faces can be a problem with this arrangement but an effective way to overcome this is to use very light-weight mirrors held in place against the crystal by the surface tension of a drop of liquid (e.g. refs. [9,10]). However this method

Using eq. (7) with the standard Nd:YAG values $\sigma = 3.5 \times 10^{-23}$ m$^2$ and $\tau_{fl} = 230$ μs and assuming the guided pump spot size to be the same as that of the signal we deduce a value for the single pass loss $L$ of 0.013. This is approximately twice that found as the upper limit for the propagation loss in our longitudinally pumped experiments. This is probably due to increased losses associated with the butting of the large plane mirrors used to form the cavity as described earlier. This would suggest that with coated end faces at least a factor of two improvement in threshold could be expected. The profile shown in fig. 3 was observed to change at higher pump powers becoming much broader and multimode in the unguided plane. Methods of maintaining a fundamental mode profile will be discussed later.

The output efficiency of this laser was tested by replacing one of the high reflectivity mirrors with a 90% reflectivity output coupler. The results for output versus input power are shown in fig. 4. The threshold has increased to a value of 48 mW in good agreement with the predictions of eq. (7) (41 mW), and a slope efficiency of ~19% is obtained. This is near to the optimum value for 590 nm pumping predicted from eq. (8) (~23%) although it should be noted that the theory assumes a single mode laser profile.

Having successfully demonstrated side-pumped waveguide laser operation with a dye laser pump the more interesting situation of diode array pumping was investigated. The 500 mW, 10 stripe, diode array (SDL-2432-H1) was collimated in the diffraction-limited (vertical) plane with a 6 mm focal length lens. A 15 cm cylindrical lens was needed to give further collimation in the horizontal plane. The resultant beam was focused, as shown in fig. 2, with a 10 cm focal length cylindrical lens such that a 8 μm (vertical) by 1.95 mm (horizontal) spot was produced at the side face of the waveguide. Using the same cavity configuration described above a threshold launched power (assuming 100% launch efficiency) of 19 mW was obtained when using high reflectivity mirrors. The threshold is higher than that obtained by dye laser pumping despite the use of lower energy photons. This is due to the longer absorption length (measured to be ~730 μm) at this wavelength, ~807 nm, leading to a worse overlap with the laser mode which, near threshold, is similar in size and location to that found previously. The discrepancy between the observed threshold value of 19 mW and that calculated from eq. (7) (10 mW) is likely to be due to having a launch efficiency lower than the assumed 100%. Once again the output profile becomes elongated and multimode in the horizontal dimension for larger pump powers.

With a 90% reflectivity output coupler the output versus input power behaviour of this diode-array side-pumped system was as shown in fig. 4. The slope efficiency of just 7% is worse than that found with dye laser pumping (~19%) despite the more favourable energy difference between the pump and signal photons. To achieve the optimum slope efficiency predicted from eq. (8) (~31%) it would be necessary for the output to have an unguided spot size of ~610 μm due to the long absorption length. In practice such a large mode size may have incurred extra losses due to non-uniformity of the crystal polishing and mirror butting over this length. One solution to this problem would be to use a higher Nd concentration. In fact it has been shown that the epitaxial growth technique can allow significantly higher

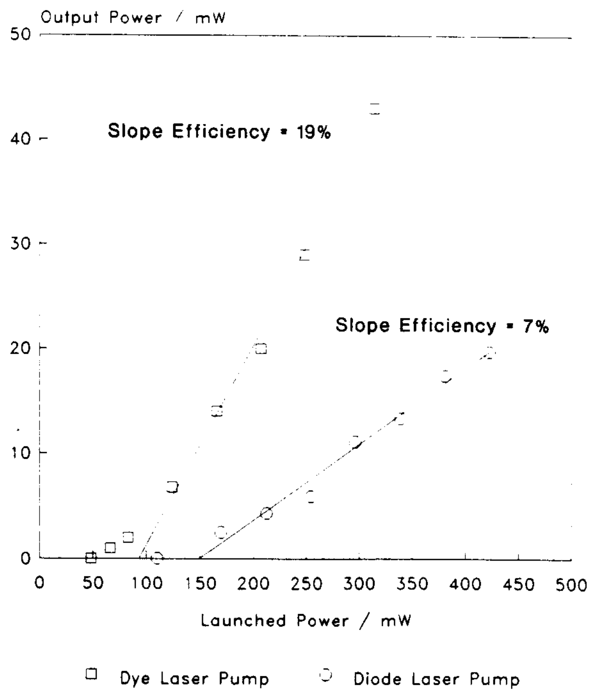


Fig. 4. Output versus input power for the dye and diode-array side-pumped waveguide laser.

concentrations to be incorporated successfully. The higher concentration should allow the optimum slope efficiency to the approached. The higher concentration also leads to concentration quenching, however in principle this should not affect the slope efficiency, and furthermore the resultant increase in threshold would be offset by the decrease in threshold due to the shorter absorption length as described earlier. Pumping a guide of appropriate width from both sides to give a more uniform excitation profile should also give higher efficiencies.

With the plane–plane resonator we have used it was to be expected that operation would become multi-transverse mode at higher output powers. However a number of steps could be taken to enforce single mode operation. The fabrication of a broad channel guide, with an appropriately chosen Nd concentration to allow efficient use of the pump light, would help the lateral confinement. Alternatively, the use of an external resonator, with cylindrical optics to couple the light from a waveguide to a separate resonator mirror or a multipass, zig-zag path, would be further options.

## 5. Conclusions

We have demonstrated the first side-pumped crystal waveguide laser. This technique should be scalable to high output power by increasing the guide length, allowing pumping by large diode arrays or bars. Direct coating of the waveguide end faces and increasing the doping level to achieve a pump absorption length closely matched to the unguided laser mode size, should give thresholds of a few milliwatts and allow high output slope efficiencies to be obtained. Further improvement in the slope efficiency may be achieved by producing a more uniform inversion distribution either by pumping from both sides or by reflecting the pump after approximately half an absorption length. The results achieved to date are in good agreement with theoretical expectation, with thresholds as low as ~8 mW and slope efficiencies of ~19%. These results are also a further indication of the high quality of the waveguide produced by the liquid phase epitaxial growth technique.

## Acknowledgements

This research is supported by the U.K. Science and Engineering Research Council (SERC) and the French CEA. A.C.L. is supported by an SERC research studentship and D.P. is supported by a CEA research studentship. We also gratefully acknowledge B. Chambaz and B. François for preparation of the waveguide samples, and S.J. Field, Ch. Wyon and J.C. Vial for useful discussions.

## Appendix

The factors $k$ and $k'$ contained in the expressions for threshold and slope efficiency are given by

$$k=\operatorname{erf}\left(\frac{\sqrt{2}d}{W_{py}}\right)\left[\operatorname{erf}\left(\frac{\sqrt{2}l}{W_{Lx}}-\frac{\sqrt{2}a}{W_{Lx}}\right)+\operatorname{erf}\left(\frac{\sqrt{2}a}{W_{Lx}}\right)\right]$$
$$\times\operatorname{erf}\left[\sqrt{2}d\left(\frac{1}{W_{py}^2}+\frac{1}{W_{Ly}^2}\right)^{1/2}\right]^{-1}$$
$$\times\left[\operatorname{erf}\left(\frac{\sqrt{2}l}{W_{Lx}}-\frac{\sqrt{2}a}{W_{Lx}}+\frac{\alpha_p W_{Lx}}{\sqrt{8}}\right)\right.$$
$$\left.+\operatorname{erf}\left(\frac{\sqrt{2}a}{W_{Lx}}-\frac{\alpha_p W_{Lx}}{\sqrt{8}}\right)\right]^{-1}$$

and

$$k'=\frac{1}{2}\left\{\operatorname{erf}\left[d\sqrt{2}\left(\frac{1}{W_{py}^2}+\frac{1}{W_{Ly}^2}\right)^{1/2}\right]\right\}^2$$
$$\times\left[\operatorname{erf}\left(\frac{\alpha_p W_{Lx}}{\sqrt{8}}+\frac{\sqrt{2}l}{W_{Lx}}-\frac{\sqrt{2}a}{W_{Lx}}\right)\right.$$
$$\left.-\operatorname{erf}\left(\frac{\alpha_p W_{Lx}}{\sqrt{8}}-\frac{\sqrt{2}a}{W_{Lx}}\right)\right]^2$$
$$\times\left\{\operatorname{erf}\left(\frac{\sqrt{2}d}{W_{py}}\right)\operatorname{erf}\left[d\sqrt{2}\left(\frac{1}{W_{py}^2}+\frac{2}{W_{Ly}^2}\right)^{1/2}\right]\right\}^{-1}$$
$$\times\left[\operatorname{erf}\left(\frac{\alpha_p W_{Lx}}{4}+\frac{2l}{W_{Lx}}-\frac{2a}{W_{Lx}}\right)\right.$$
$$\left.-\operatorname{erf}\left(\frac{\alpha_p W_{Lx}}{4}-\frac{2a}{W_{Lx}}\right)\right]^{-1}.$$

These can be important if we wish to consider the optimum value for $W_{Lx}$. For instance, if we did not include $k$ in eq. (7) then a threshold power of zero could be obtained for $W_{Lx}=\infty$. If we include $k$ a non zero optimum value of threshold is obtained for $W_{Lx}=0$. In practice a value greater than zero is obtained as we have not accounted for diffraction in these equations.

## References


[1] P.W. France, ed., Optical fibre lasers and amplifiers (Blackie, London, 1991).

[2] G. Huber and K. Petermann, Tunable solid state lasers, eds. P. Hammerlig, A.B. Budgor and A. Pinto (Springer, Berlin, 1985) p. 11.

[3] S.A. Payne, L.L. Chase, H.W. Newkirk, L.K. Smith and W.F. Krupke, IEEE J. Quantum Electron. QE-24 (1988) 2243.

[4] P.F. Moulton, J. Opt. Soc. Am. B 3 (1986) 125.

[5] A.J. Silversmith, W. Lenth and R.M. Macfarlane, Appl. Phys. Lett. 51 (1987) 1977.

[6] S.A. Pollack, D.B. Chang and M. Birnbaum, Appl. Phys. Lett. 54 (1989) 869.

[7] T.Y. Fan, A. Cordova-Plaza, M.J.F. Digonnet, R.L. Byer and H.J. Shaw, J. Opt. Soc. Am B 3 (1986) 140.

[8] E. Lallier, J.P. Pocholle, M. Papuchon, Q. He, M. De Micheli, D.B. Ostrowsky, C. Grezes-Besset and E. Pelletier, Electron. Lett. 27 (1991) 936.

[9] S.J. Field, D.C. Hanna, A.C. Large, D.P. Shepherd, A.C. Tropper, P.J. Chandler, P.D. Townsend and L. Zhang, Opt. Lett. 17 (1992) 52.

[10] S.J. Field, D.C. Hanna, A.C. Large, D.P. Shepherd, A.C. Tropper, P.J. Chandler, P.D. Townsend and L. Zhang, Electron. Lett. 27 (1991) 2375.

[11] E. Lallier, J.P. Pocholle, M. Papuchon, M. De Micheli, M.J. Li, Q. He, D.B. Ostrowsky, C. Grezes-Besset and E. Pelletier, IEEE J. Quantum Electron. QE-27 (1991) 618.

[12] R. Brinkmann, W. Sohler and H. Suche, Electron. Lett. 27 (1991) 415.

[13] M.J.F. Digonnet, C.J. Gaeta, D. O'Meara and H.J. Shaw, J. Lightwave Technol. LT-5 (1987) 642.

[14] D. Pelenc, B. Chambaz, I. Chartier, B. Ferrand and J.C. Vial, in: Digest of Laser M2P (Université Joseph Fourier, Grenoble, 1991) paper E40.

[15] I. Chartier, B. Ferrand, D. Pelenc, S.J. Field, D.C. Hanna, A.C. Large, D.P. Shepherd and A.C. Tropper, Growth and low threshold laser oscillation of an epitaxially grown Nd:YAG waveguide, Optics Lett. submitted.

[16] H. Po, E. Snitzer, R. Tumminelli, L. Zenteno, F. Hakimi, N.M. Cho and T. Haw, in: Proc. of Conference on Optical fibre communications (Optical Society of America, Washington, D.C., 1989) paper PD7.

[17] T.M. Baer, D.F. Head and M. Sakamoto, in: Digest of Conference on Lasers and electro-optics (Optical Society of America, Washington, D.C., 1989) paper FJ5.

[18] W.A. Clarkson and D.C. Hanna, J. Mod. Optics 36 (1989) 483.